Transparent counter electrodes for Bifacial dye-sensitized solar cells: A Review

[1]Jothika B, [2]Mrunal Deshpande, [3]R.Govindaraj

[1]JRF, [2]Associate Professor, [3]Assistant Professor
[1,2]Electricals and electronics engineering, [3] Department of physics
[1] Sri Sivasubramaniya Nadar college of engineering, Kalavakkam, Chennai, India

Abstract : Over the following ten years, it is anticipated that the market share of bifacial solar cells would rise due to the increased power produced per area. In bifacial solar cells more dye molecules are stimulated and more carriers are produced as a result of the sunlight being irradiated from both the front and back simultaneously, increasing short-circuit current density and, consequently, overall conversion efficiency. The main components of Bifacial dye sensitized solar cell (BFDSSC) include titanium dioxide/metal oxide-based photo anode, dye, an electrolyte and a counter electrode. In evaluating the overall effectiveness of a BFDSSC device, the counter electrode plays an important role. Platinum is the most commonly used material for CE. Due to its high cost and limited availability, considerable efforts have been made to identify less expensive replacements. This article provides a concise overview of the materials used for counter electrodes in BFDSSCs with their merits and drawbacks.

IndexTerms - **Transparent counter electrodes, Bifacial DSSC, platinum free**

I. INTRODUCTION

Solar cells have been at the centre of the present low-carbon economy and have sparked an increase in interest in the field of environmental and energy applications due to the depletion and pollution of fossil fuels. The most effective method of solar energy conversion is the photovoltaic technique. Compared to manufactured silicon solar cells. The photovoltaic process is the most efficient method of converting solar energy. When compared to conventional silicon solar cells, 2, 3 dye-sensitized solar cells (DSSCs) have appealing advantages in terms of ease of manufacture, zero-emission, and cost-effectiveness. [1−5] So far, the DSSC device with a Co(II/III)tris(bipyridyl) based redox electrolyte, a platinum (Pt) counter electrode (CE), and a zinc porphyrin dye-sensitized TiO_2 anode has achieved the highest efficiency of 12.3 percent. [6] Han et al. previously validated a conversion efficiency of 11.1 percent by sandwiching a liquid electrolyte comprising I/I_3 redox couples between a black dye-sensitized TiO_2 and a Pt CE [7].

In the last two decades, DSSCs have been aggressively studied as a possible alternative light-harvesting technology. The reduced production cost, ease of fabrication, transparency, colour tunability, flexibility of integration onto diverse substrates, and significantly greater power conversion efficiencies (PCEs) in diffused/artificial light circumstances have all contributed to DSSCs' continuing popularity. All of these measurements are the result of front irradiation (irradiated from TiO_2 anode). Because to an increased loss of incident light within the dye-sensitized TiO_2 film, irradiation and hence excitation of dye molecules are incomplete, resulting in a low electron density on the TiO_2nanocrystallite's conduction band (CB) [11,12]. It is not unusual to find a substantially lower efficiency than the theoretical number.

Ito et al. proposed bifacial dye-sensitized solar cells (BF-DSSCs) in 2008 [13], and they have received a lot of attention recently due to their irradiation of sunlight from both sides, which considerably boosts the solar energy utilisation ratio and simplifies installation of solar cell [14,15]. Furthermore, the two-sided transparency allows BF-DSSCs to be used as a portable battery and in building integrated photovoltaic systems, where BF-DSSCs should be merged with transparent substrates such as skylights, building windows, panel screens, and lampshades [13]. As a result, designing and fabricating transparent catalytic counter electrodes (CEs) with high electro catalytic activity for Bi-DSSCs is critical.

DSSC's bifacial design can help reduce the cost of solar to electric energy conversion by providing front and back illumination [2]. Light incidence from the photo anode side causes front lighting, whereas light incidence from the counter electrode causes rear illumination. One of the most significant advantages of employing bifacial designs is the ability to create building integrated photovoltaics. When paired with reflecting devices, bifacial solar cells can produce more electrical power [4]. To obtain efficient bifacial DSSCs, the DSSC counter electrode must be transparent or semi-transparent. Previous research has shown that employing thinner or porous platinum sheets, counter electrodes can be transparent or semi-transparent [5]. Due to the high cost and scarcity of platinum [7], [8], many efforts have been made to construct low-cost Pt-free counter electrodes employing carbon materials [10–17], conducting polymers [18–20], and inorganic compounds [21–23]. Transparent metal selenide alloy counter electrodes (CuSe, NiSe, CoSe, FeSe, and RuSe) have recently been reported to have higher rear efficiency than platinum counterparts [24].

Obtaining high transparency, high conductivity, and appropriate catalytic activity from a single material is difficult. As a result, composite materials such as MoS_2-graphene Nano sheet, grapheme /PEDOT/PSS and PANI/Reduced Graphene oxides [25], [26] have been reported. However, the performance of Pt-free counter electrodes is limited due to insufficient catalytic activity.

Because of their ability to adjust both colour and transparency at the same time, bifacial DSSCs have emerged as one of the leading options in Building Integrated Photovoltaic (BIPV) technology. Counter electrodes play a vital role in catalytic activity. To make the solar cell transparent as well as efficient the following features must be considered while choosing a material for the counter electrode.

II. FEATURES OF THE COUNTER ELECTRODES

One of the most significant components of BF-DSSCs is the counter electrode (CE). The CE's primary function is to either (a) operate as a catalyst by reducing redox species, which are mediators for regenerating the sensitizer (dye) after electron injection, or (b) collect the hole from hole-transporting materials in a solid-state solar cell. The majority of BFDSSC research focuses on enhancing efficiency by raising the short-circuit current density (J_{SC}), open-circuit voltage (V_{OC}), and fill-factor (FF). The redox species utilized to transfer electrons between the dye adsorbed photo anode and the CE determines the reactions at the CE. In DSSCs, the redox mediator is often an I^-/I_3^- couple. The reaction mentioned in equation 1 reduces the I_3^- produced as a result of dye renewal at the counter electrode.

$$I_3^- + 2e \rightarrow 3I^- \tag{1}$$

Figure 1 depicts the features of high-performance CEs. When an ineffective CE is used, which gives high resistance via slow reaction, the performance of BF-DSSCs suffers dramatically. The CE material must be chosen based on the BF-DSSC's specific use. In a BF-DSSC, a CE material should have high catalytic activity and be stable to the electrolyte employed in the cell. Pt is a common choice for CE in BF-DSSCs due to its appealing qualities such as strong catalytic activity, high performance and transparency [32–34]. It is frequently used as the active material in BF-DSSCs.
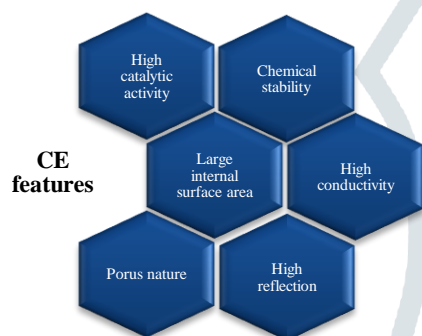
However, Pt is a costly noble metal, and it must be replaced with less expensive materials in order for BF-DSSCs to be commercialized. Carbon nanostructures, activated carbon, CNTs, graphene, conducting polymers, and other materials, in various combinations, have been used as CE materials, and transition metal carbides, nitrides, sulphides, and oxides have recently been evaluated as CE materials due to their availability, plasticity, and ease of fabrication.

Some conducting polymers showed promise as CEs; for example, PEDOT has excellent catalytic characteristics. The performance of the polymer CE-based DSSCs, on the other hand, fell short of the required degree of efficiency. Finally, carbon CE was introduced as a low-cost material that may be predicted to be used in low-cost, high-energy production devices in the future.

Transition-metal nitrides and carbides are widely used in a variety of sectors, and many of them show good catalytic activity for the reduction of triiodide ions. In order to produce unique counter electrodes for DSSCs, much research is required with new concept or design strategy. When creating or constructing counter electrode materials, we should keep in mind that it should be inexpensive, environmentally safe, and good transparency and high electro catalytic activity.

However, in order to fabricate CEs for BF-DSSCs, a number of problems must be addressed. Further research into new low-cost materials for CEs with reasonable catalytic activity is required. Because of their simplicity of manufacture and reduced material usage, third-generation emerging technologies are attracting a lot of attention. Fabrication costs are lower with BF-DSSCs since transparent electrodes are used and both electrodes are solid films. The availability of a wide range of TiO_2 materials with outstanding stability contributes to the inexpensive cost of photo anodes. CEs, on the other hand, are costly because of the usage of expensive materials such as platinum, metal oxides, and conducting polymers.

As transparent CEs for Bi-DSSCs, conductive polymers such as poly(3,4-ethylenedioxythiophene) [10], polyaniline [11], and polypyrrole (PPy) [12–14] have been used. Among these conductive polymers, PPy has been identified as the most promising transparent CE material due to its ease of synthesis, high catalytic activity and stability, and great transparency [12].

In this review article, we are discussing the different transparent counter electrode materials which can be used as a replacement for platinum-based CEs.

III. PEDOT COUNTER ELECTRODES

Abdelaal S.A. Ahmedet al. [28] used a solvothermal technique to create a Si_3N_4/MoS_2 nanocomposite, which was then mixed with polystyrene sulfonate-doped poly (3, 4-ethylenedioxythiophene) to create Si_3N_4/MoS_2-PEDOT: PSS as a counter electrode for bifacial DSSCs. Electrochemical experiments show that Si_3N_4/MoS_2-PEDOT: PSS CEs have higher catalytic activity than virgin Si_3N_4/MoS_2 and PEDOT: PSS. The conversion efficiency of the DSSCs with 5% Si_3N_4/MoS_2-PEDOT: PSS composite CE is 7.16 %, which is almost equivalent to the standard platinum CE (7.50 %) and better than the pristine Si_3N_4/MoS_2 (3.80 %) or PEDOT: PSS (4.20 %) CEs. Because of the optical transparency of Si_3N_4/MoS_2-PEDOT: PSS composite CEs, bifacial DSSCs based on 5% Si_3N_4/MoS_2-PEDOT: PSS CE yields 2.03% PCE in rear irradiation.

They got the XRD patterns of MoS_2which revealed a strong diffraction peak at $2\theta=15.0°$ corresponding to the (0 0 2) crystal plane, indicating the stacked layered structure of crystalline MoS_2, as well as four broad diffraction peaks at $2\theta=32.6°$, $35.7°$, $44.3°$, and $57.6°$ for the (1 0 0), (1 0 2), (0 0 6) and (1 1 0) planes of hexagonal MoS_2.X-ray photoelectron spectroscopy (XPS) was used to further analyse the composition of Si_3N_4/MoS_2. The results validated the successful preparation of the Si_3N_4/MoS_2 composite.

FESEM was used to examine the surface morphologies of PEDOT: PSS, Si_3N_4/MoS_2-PEDOT: PSS, and Si_3N_4/MoS_2 films. The FESEM cross-sectional images of PEDOT: PSS and Si_3N_4/MoS_2-PEDOT: PSS CEs were obtained and analysed, revealing that the deposited films have good adhesion to the FTO substrates and that the mean film thicknesses of PEDOT: PSS and Si_3N_4/MoS_2-PEDOT: PSS composite films are 94 and 550 nm, respectively. According to the cross-sectional SEM picture, the thickness of the produced Pt CE was 571 nm. Energy dispersive X-ray (EDX) elemental analysis revealed the matching elements of Si_3N_4/MoS_2in PEDOT: PSS matrices.

Because the CE's primary purpose is to catalyse the reduction of I_3^-, the peak current density (J_{pc}) and peak-peak separation (E_{pp}) of the more negative redox peak are utilised to determine the CE's catalytic activity (Peng et al., 2012; Zheng et al., 2014a, b) [29,30].In comparison to PEDOT:PSS and Si_3N_4/MoS_2, Si_3N_4/MoS_2-PEDOT:PSS exhibits higher Jpc and lower Epp, indicating improved catalytic activity. The prepared DSSC, which uses 5% Si_3N_4/MoS_2-PEDOT: PSS CE with 520 nm thicknesses, not only has a greater conversion efficiency of 7.16 % than PEDOT: PSS and Si_3N_4/MoS_2but also has a 2.03 % from rear illumination. Because of the transparency of conversion efficiency and the low temperature of the fabricated DSSCs, it is a good option to replace the expensive Pt-based CE in large-scale applications.

Fadzai Lesley Chawarambwa et al. [32] reported PEDOT: PSS/DMSO/TX100/TiO_2 CE, having Iso-octyphenoxy-polyethoxyethanol (TX100) i.e. Triton X-100, DMSO, and TiO_2 combination with PEDOT: PSS. A bifacial DSSC based on the PEDOT: PSS/DMSO/TX100/TiO_2 CE was created, and its photovoltaic properties were measured under 100 mWcm^{-2} simulated solar light. Triton X is a surfactant that is commonly used to improve the film porosity of many materials [33]. Choi et al. [34] previously used Triton X-100 to enhance the conductivity of PEDOT: PSS films by stabilising the PEDOT nanoparticles. PEDOT: PSS was combined with dimethyl sulfoxide (DMSO), iso-octyphenoxy-polyethoxyethanol, and trace amounts of TiO_2 nanoparticles to create a novel CE. They also test the new material's transmittance, conductivity, internal resistance, and electro catalytic activity.

The surface of the PEDOT: PSS and PEDOT: PSS/DMSO/TX100/TiO_2 films are homogeneous and smooth. The PEDOT: PSS/DMSO/TX100/TiO_2 film is more porous than the PEDOT: PSS film, as evidenced by the miniature holes that are spread across the surface of the film; as a result, more catalytic active sites are available, resulting in more effective iodide/triiodide (I^-/I_{3-}) reduction reactions [35-37]. This structure strengthens the contact with the FTO glass and improves electrolyte permeability [38]. As a result, the authors found that the combination of TiO_2 nanoparticles and iso-octyphenoxy-polyethoxyethanol can improve the porosity and surface area of PEDOT: PSS.

The transmittance of the CE film affects the photovoltaic performance of the DSSC because incident light must travel through the CE film before being focused on the TiO_2 light-harvesting layer. The CE transmittance was measured between 300 and 800 nm. The authors' findings revealed that the PEDOT: PSS/DMSO films had the maximum transmittance, followed by the PEDOT: PSS/DMSO/TX100/TiO_2 and Pt films. This is achievable because of the high transmittance of Triton X-100 [39] and PEDOT: PSS [40] at visible wavelengths.

As in earlier research, cyclic volt ammetry (CV) was used to measure electro catalytic activity at a scan rate of 100 mVs^{-1} in the potential range of -2 to 2 V. According to the results, PEDOT: PSS-based CE has the highest Z1 (First semicircles internal impedance associated with the charge transportation at the CE/electrolyte interface 11.80Ω) and Z2 (Second semicircles internal impedance related to the charge transfer at the photo anode/electrolyte interface74.81Ω). The PEDOT: PSS/DMSO/TX100/TiO_2 CE, on the other hand, has a low Z1 (4.017Ω) and Z2 (28.67Ω). This suggests that the inclusion of Triton X-100 and TiO_2 nanoparticles increases conductivity. The Z1 resistance of the PEDOT: PSS/DMSO/TX100/TiO_2 as CE (4.017Ω) was lower than that of the Pt-based CE (4.615Ω), showing that electron transport increased at the CE/electrolyte interface. PEDOT: PSS/DMSO/TX100/TiO_2 and Pt CEs both have low total resistances, indicating that they are very conductive.

The FF of the DSSC with PEDOT: PSS/DMSO (0.67) was much lower (because of the flatness and smaller surface area of the PEDOT: PSS/DMSO CE) than that of the DSSC with PEDOT: PSS/DMSO/TX100/TiO_2 (0.68). The DSSC with the Pt CE, on the other hand, has a Jsc of 4.539mAcm^{-2} and a fill factor of 0.69, which are both lower than those of the DSSC with the PEDOT: PSS/DMSO/TX100/TiO_2 and PEDOT: PSS/DMSO based CE. The total efficiency under bifacial illumination was 9.14 % for DSSCs made with the PEDOT: PSS/DMSO/TX100/TiO_2 based CE and 8.66 % for DSSCs made with the Pt based CE, respectively. The results show that the prepared PEDOT: PSS/DMSO/TX100/TiO_2 CE can be used in place of traditional Pt-based CEs in future bifacial DSSCs.

Jin Soo Kang et al. [41] reported a combination of electro polymerized poly(3,4-ethylenedioxythiphene) (PEDOT) counter electrodes and cobalt bipyridine redox ($[Co(bpy)_3]^{3+/2+}$) electrolyte. They mention that both these materials demonstrated higher transparency compared to that exhibited by standard Pt and iodide counterparts. To regulate the thickness these authors have used electro polymerization approach to manufacture PEDOT films. They further observed that these PEDOT CE developed in such a way decrease the thickness of the film and has low ohmic resistance resulting into more active PEDOT. A specific procedure was used and Monomeric 3,4-ethylenedioxythiphene (EDOT) was electro polymerized onto fluorine-doped tin oxide (FTO) glass substrates at a scan rate of 50 mV/s at potential cycles of certain range. By varying the number of potential cycles, the three electrodesPEDOT 1, PEDOT 2, and PEDOT 3 were developed.

SEM micrographs reveal that overall morphologies of the PEDOT films were identical to that of the FTO glass substrate indicating homogeneous deposition of PEDOT films with electro-polymerization. Cross-sectional SEM images produced by focused ion beam (FIB) milling gave the thicknesses of the PEDOT electrodes.

The authors used Cyclic voltammetry (CV) studies to evaluate the electro catalytic activity of the PEDOT CEs in both iodide and cobalt bipyridine redox electrolytes. To represent electro catalytic activity of the CEs for DSSC applications reduction currents measured at a very low potential was used. The results of using this reduction current were almost identical for both Pt and PEDOT CEs, which shows that the electro catalytic activities of both in iodide redox electrolyte is similar.

With the increase in thickness of the PEDOT, the smaller series resistance (Rs) values increased but weakened the electrical conductivity of PEDOT as compared to the FTO substrate. But for better electrical properties, thinner film gives good results as ohmic resistance reduces with thickness during electron transmission from the conductive FTO substrate to the surface of the PEDOT layer.

In the case of the PEDOT 1 CE, η values of 7.40 % (front) and 5.23 % (back) were reported. The thickness of PEDOT also affected the performance of NI-DSSCs as with thick films have higher ohmic resistance and also increased photon loss at CEs.

The authors [41] also observed that the retention rate of 86.5 % for η was among the best results from state-of-the-art bifacial DSSCs, and the performance of DSSC demonstrated the highest efficiency among bifacial DSSCs under back-illumination operation conditions. With this it was suggested that a cell architecture based on a very uniform and thin PEDOT CE and cobalt bipyridine redox electrolyte is a viable technique for achieving excellent performance in bifacial DSSCs.

With their high transparency in the visible light wavelength region and favourable optical mismatch with sensitizers, PEDOT CEs significantly improved the overall performance of the bifacial DSSCs as compared to traditional Pt CEs. High retention under back illumination for bifacial DSSC was thus noticed due to the excellent electro catalytic activity of PEDOT films in cobalt bipyridine redox electrolytes.

IV. POLYOXOMETALATE MODIFIED TRANSPARENT METAL SELENIDE COUNTER ELECTRODES

Lu Zhang, et al. [42] proposed a straightforward one-step technique for in situ synthesis of PW_{11} Co polyoxometalates on graphene-like $Co_{0.85}Se$ (abbreviated as PW_{11} Co-n/$Co_{0.85}Se$, where n represents the concentration of $PW_{11}Co$). Metal selenides, particularly cobalt selenide (CoSe), are expected to create effective and stable bifacial DSSCs due to their distinctive platinum-like electrical structure, good optical transparency, low cost, and tolerable electro catalytic activity. Cobalt selenides with various morphologies (e.g., Nano rods, Nano belts, petal-like Nano sheets, and hollow nanoparticles) have been found and efficiently assessed in bifacial DSSCs with accessible triiodide reduction activity. Surprisingly, it is discovered that the pioneering example of DSSCs based on CoSe CEs with significant power conversion efficiency is based on their unusual two-dimensional graphene-like shape.

Polyoxometalates (POMs) are a well-known polynuclear nano-size metal-oxo cluster with distinct structures and broad characteristics. Because of their tuned molecular design and sizes, good thermal stabilities and solubility, low cost, and mild preparation conditions, such nanoscale clusters are regarded as "guest" species to be combined with various 2D materials (for example, MoS_2, graphene, and carbon nitride polymers) to give rise to composite materials with target functionalities, particularly POM-based transparent composite films.

It is obvious from the SEM image of PW Co/$Co_{0.85}Se$ grown in situ on an FTO substrate that the leaf-shaped PW Co/ $Co_{0.85}Se$ was successfully grown on the FTO substrate. The greater the transparency, the lesser the surface coverage. The inclusion of POMs increased the surface coverage of selenides on FTO compared to the original CoSe, but the transparency of PW Co/Co Se remained nearly unchanged.

The PCE and Jsc values of the DSSC's front illumination are 5.89 % and 14.40 mA/cm², respectively, but the back illumination is reduced to 4.47 % and 11.87 mA/cm², respectively. When Pt was replaced with $Co_{0.85}SeCE$, the PCE and Jsc were dramatically enhanced to 6.45 % and 15.80 mA/cm² by front irradiation, respectively, and 5.33 % and 13.26 mA/cm² by back irradiation. As a result, while $Co_{0.85}Se$ performs similarly to Pt in front lighting, it outperforms Pt in back lighting because to its high transmittance.

As a result, $Co_{0.85}Se$ has a promising future in bifacial DSSCs. To regulate the characteristics of $Co_{0.85}Se$ materials, authors added $PW_{11}Co$ with varying amounts. The inclusion of POMs had no effect on the transmittance of selenide... Notably, the PCE and Jsc values of the DSSC's front illumination based on the PW Co-0.5/$Co_{0.85}Se$ CE are 7.56 % and 16.03 mA/cm², respectively, and 5.82 % and 13.18 mA/cm², respectively. However, when the POM content increases, the photoelectric characteristics of DSSCs diminish. As a result, the POM content has a considerable effect on the catalytic activity of selenide.

V. CoSe₂ NANO ROD COUNTER ELECTRODE

Juan Xia et al. [43] used a simple hydrothermal process to generate $CoSe_2$ Nano rods with lengths of 70–500 nm and widths of 20–60 nm, which served as the counter electrode material. $CoSe_2$ CE, as an essential form of selenide, has tremendous potential due to its excellent electro catalytic activity for I_3^- reduction, low cost, and ease of manufacture. $CoSe_2$ CE has demonstrated excellent photoelectric efficiency in previous investigations; however, all of the research have primarily focused on liquid electrolytes, and hence the DSSCs have encountered the problem of instability due to evaporation and leakage of the liquid solvent [29]. The authors devised an approach that uses a quasi-solid-state gel electrolyte to improve the long-term stability of DSSCs.

XRD pattern show the acquired $CoSe_2$ with the principal diffraction peaks at 2θ=30.7, 34.6, 35.9, 47.7, 53.4, and 63.3 corresponding to the (101), (111), (120), (031), and (122) crystal faces of $CoSe_2$, which can be entirely matched with the orthorhombic structure of $CoSe_2$. They used an energy dispersive X-ray spectroscope (EDS) to map the element distribution of the $CoSe_2$ Nano rods. From the relevant region of the SEM micrograph, the mapping images show a homogeneous distribution of Se and Co elements in the $CoSe_2$ Nano rod structure.

The front PCE of the quasi-solid-state cell with the $CoSe_2$ Nano rod CE was 8.02 % and the Jsc was 15.01 mA/cm², which were greater than those of the Pt electrode (PCE = 7.46 % and Jsc = 13.78 mA/cm²). It is worth noting that the Voc value of $CoSe_2$ Nano rod CE (742 mV) is lower than that of Pt CE (773 mV), most likely due to increased backward reactions, which might result in a greater dark current and a lower Voc value.

In both the $CoSe_2$ and Pt CEs, the rear irradiation PCE and Jsc values are significantly lower than those from the front irradiation. The light intensity will progressively diminish as the rear illumination proceeds through the long process of the FTO substrate, $CoSe_2$ (or Pt) layer and quasi-solid-state electrolyte to excite the dye. It should be observed that the $CoSe_2$ rear results have a higher PCE of 4.22 % and a higher Jsc of 8.32 mA/cm² than the Pt CE results (PCE= 4.04 % and Jsc= 7.88 mA/cm²). In the visible-light region, the $CoSe_2$ CE has better optical transparency (88%) than the typical Pt electrode (83%). This finding implies that scattering and reflection light can pass through the $CoSe_2$ layer and electrolyte for reabsorption by the N719 dye, resulting in a higher rear irradiation efficiency than Pt.

Table 1: Performance of different CEs for Bifacial dye-sensitized solar cells

CEs	Irradiation	Voc(mV)	Jsc(mAcm^{-2})	FF	PCE(%)	Ref
Pristine PEDOT: PSS	Front	0.73	11.89	48.19	4.2	
	Rear	0.71	3.99	83.27	2.36	
10%Si$_3$N$_4$/MoS$_2$-PEDOT: PSS	Front	0.73	14.41	69.04	7.22	
	Rear	0.62	2.84	70.93	1.26	28
PEDOT:PSS/DMSO	Front	0.74	8.123	0.58	3.49	
	Rear	0.71	5.139	0.67	2.42	
PEDOT:PSS/DMSO/Triton X-100/TiO$_2$	Front	0.74	8.424	0.72	4.41	
	Rear	0.73	5.638	0.74	3.05	32
PW Co-0.3/ Co$_{0.85}$Se	Front	0.8	17.06	0.53	7.18	
	Rear	0.79	13.2	0.54	5.63	
PW Co-0.5/ Co$_{0.85}$Se	Front	0.84	16.03	0.56	7.56	
	Rear	0.76	13.18	0.58	5.82	42
PEDOT and([Co(bpy)$_3$]$^{3+/2+}$)	Front	0.872	14.5	0.68	8.65	
	Rear	0.876	11.9	0.71	7.48	41
CoSe$_2$	Front	0.742	15.01	0.72	8.02	
	Rear	0.715	8.32	0.71	4.22	43

The electrochemical stability of CE material is an important factor in the actual application of BQDSSCs (bifacial and quasi-solid-state cells) devices. To assess it, the two symmetrical cells containing CoSe$_2$ and Pt CEs underwent successive CV scanning and sequential EIS (Electrochemical impedance spectroscopy) tests. In comparison to Pt CE, the peak current density and Epp of CoSe$_2$ CE did not vary significantly after 30 cycles, indicating that CoSe$_2$ has high electrochemical stability. Furthermore, after 10 cycles of EIS scanning, there are essentially no changes in Rs (Series resistance) and ZN (Nernst diffusion impedance) for the two cells, implying that potential cycling has a negligible effect on series resistance and mass transfer in the redox electrolyte solution [54,58].

When compared to the Pt CE, the CoSe$_2$ Nano rod CE has a larger specific surface area, a lower charge transfer resistance, and a faster charge transfer rate, all of which help to boost the electro catalytic activity towards I$_3^-$ reduction in the polyvinylidene fluoride (PVDF)quasi-solid-state electrolyte. CoSe$_2$ Nano rods demonstrated remarkable front and back PCEs of 8.02 % and 4.22 % in BQDSSCs, which were superior to Pt CE. The CoSe$_2$ CE, in particular, demonstrated quick photocurrent responsiveness and long-term photovoltaic stability. Furthermore, CoSe$_2$ CE demonstrates remarkable electrochemical stability in subsequent CV scanning and EIS measurements.

We here summarized the different counter electrode material performance for bifacial dye-sensitized solar cells. The performances of the different materials are listed in table 1.

VI. CONCLUSION

We can conclude that for BFDSSCs, the practicality of several CE materials has been established by various authors. The counter electrode, as a crucial component of DSSCs, collects electrons from the external circuit and catalyses the redox reduction in the electrolyte, which has a significant influence on the photovoltaic performance, long-term stability and cost of the devices. bifacial dye-sensitized solar cell structure that provides high photo-energy conversion efficiency (similar to 6%) for incident light striking its front or rear surfaces. The design comprises a highly stable ruthenium dye in combination with an ionic-liquid electrolyte and a porous TiO2 layer. The inclusion of a SiO2 layer between the electrodes to prevent generation of unwanted back current and optimization of the thickness of the TiO2 layer are responsible for the enhanced performance. The DSSC has a number of attractive features; it is simple to make using conventional roll-printing techniques, is semi-flexible and semi-transparent which offers a variety of uses not applicable to glass-based systems, and most of the materials used are low-cost. In practice it has proven difficult to eliminate a number of expensive materials, notably platinum and ruthenium, and the liquid electrolyte presents a serious challenge to making a cell suitable for use in all weather. The DSSC with PEDOT/Si$_3$N$_4$/MoS$_2$, PEDOT /DMSO/TX100/TiO$_2$, or PEDOT CE with cobalt bipyridine redox ([Co(bpy)3]3$^+$/2$^+$) electrolyte can achieve PCE values of more than 7%. Nonetheless, more study on the mechanism of I$_3^-$ reduction over PEDOT-based composite CEs or other materials is required to explain how a promoter can boost the electrode's catalytic activity. There is an interesting study area be to explore CE for DSSCs with various electrolytes. Electrodes are used in different battery types, electroplating and electrolysis, welding, cathodic protection, membrane electrode assembly, for chemical analysis, and Taser electroshock weapon. In the medical field, electrodes are also used in ECG, ECT, EEG, and defibrillator. The industrialisation of BFDSSCs applications can be speed up by maintaining transparency while concurrently having the added benefit of enhanced PCE under full sun and interior light circumstances

REFERENCES

[1] Zeng, Z., Wang, D., Wang, J., Jiao, S., Huang, Y., Zhao, S., Zhang, B., Ma, M., Gao, S., Feng, X. and Zhao, L., 2020. Self-Assembly Synthesis of the MoS$_2$/PtCo Alloy Counter Electrodes for High-Efficiency and Stable Low-Cost Dye-Sensitized Solar Cells. *Nanomaterials*, *10*(9), p.1725.

[2] Xu, T., Kong, D., Tang, H., Qin, X., Li, X., Gurung, A., Kou, K., Chen, L., Qiao, Q. and Huang, W., 2020. Transparent MoS$_2$/PEDOT composite counter electrodes for bifacial dye-sensitized solar cells. *ACS omega*, *5*(15), pp.8687-8696.

[3] Kumar, D.K., Kříž, J., Bennett, N., Chen, B., Upadhayaya, H., Reddy, K.R. and Sadhu, V., 2020. Functionalized metal oxide nanoparticles for efficient dye-sensitized solar cells (DSSCs): A review. *Materials Science for Energy Technologies*, *3*, pp.472-481.

[4] Sudhakar, V., Singh, A.K. and Chini, M.K., 2020. Nanoporous reduced graphene oxide and polymer composites as efficient counter electrodes in dye-sensitized solar cells. *ACS Applied Electronic Materials*, *2*(3), pp.626-634.

[5] Theerthagiri, J., Senthil, A.R., Madhavan, J. and Maiyalagan, T., 2015. Recent progress in non-platinum counter electrode materials for dye-sensitized solar cells. *ChemElectroChem*, 2(7), pp.928-945.

[6] Samantaray, M.R., Mondal, A.K., Murugadoss, G., Pitchaimuthu, S., Das, S., Bahru, R. and Mohamed, M.A., 2020. Synergetic effects of hybrid carbon nanostructured counter electrodes for dye-sensitized solar cells: a review. *Materials*, 13(12), p.2779.

[7] Zeng, Z., Wang, D., Wang, J., Jiao, S., Huang, Y., Zhao, S., Zhang, B., Ma, M., Gao, S., Feng, X. and Zhao, L., 2020. Self-Assembly Synthesis of the MoS_2/PtCo Alloy Counter Electrodes for High-Efficiency and Stable Low-Cost Dye-Sensitized Solar Cells. *Nanomaterials*, 10(9), p.1725.

[8] Xu, T., Kong, D., Tang, H., Qin, X., Li, X., Gurung, A., Kou, K., Chen, L., Qiao, Q. and Huang, W., 2020. Transparent MoS_2/PEDOT composite counter electrodes for bifacial dye-sensitized solar cells. *ACS omega*, 5(15), pp.8687-8696.

[9] Kumar, D.K., Kriz, J., Bennett, N., Chen, B., Upadhayaya, H., Reddy, K.R. and Sadhu, V., 2020. Functionalized metal oxide nanoparticles for efficient dye-sensitized solar cells (DSSCs): A review. *Materials Science for Energy Technologies*, 3, pp.472-481.

[10] Sudhakar, V., Singh, A.K. and Chini, M.K., 2020. Nanoporous reduced graphene oxide and polymer composites as efficient counter electrodes in dye-sensitized solar cells. *ACS Applied Electronic Materials*, 2(3), pp.626-634.

[11] Theerthagiri, J., Senthil, A.R., Madhavan, J. and Maiyalagan, T., 2015. Recent progress in non-platinum counter electrode materials for dye-sensitized solar cells. *ChemElectroChem*, 2(7), pp.928-945.

[12] Samantaray, M.R., Mondal, A.K., Murugadoss, G., Pitchaimuthu, S., Das, S., Bahru, R. and Mohamed, M.A., 2020. Synergetic effects of hybrid carbon nanostructured counter electrodes for dye-sensitized solar cells: a review. *Materials*, 13(12), p.2779.

[13] Tomar, N., Dhaka, V.S. and Surolia, P.K., 2021. A brief review on carbon nanomaterial counter electrodes for N719 based dye-sensitized solar cells. *Materials Today: Proceedings*.

[14] Rafique, S., Rashid, I. and Sharif, R., 2021. Cost effective dye sensitized solar cell based on novel Cu polypyrrole multiwall carbon nanotubes nanocomposites counter electrode. *Scientific Reports*, 11(1), pp.1-8.

[15] Younas, M., Baroud, T.N., Gondal, M.A., Dastageer, M.A. and Giannelis, E.P., 2020. Highly efficient, cost-effective counter electrodes for dye-sensitized solar cells (DSSCs) augmented by highly mesoporous carbons. *Journal of Power Sources*, 468, p.228359.

[16] Lemos, H.G., Barba, D., Selopal, G.S., Wang, C., Wang, Z.M., Duong, A., Rosei, F., Santos, S.F. and Venancio, E.C., 2020. Water-dispersible polyaniline/graphene oxide counter electrodes for dye-sensitized solar cells: Influence of synthesis route on the device performance. *Solar Energy*, 207, pp.1202-1213.

[17] Thomas, S., Deepak, T.G., Anjusree, G.S., Arun, T.A., Nair, S.V. and Nair, A.S., 2014. A review on counter electrode materials in dye-sensitized solar cells. *Journal of Materials Chemistry A*, 2(13), pp.4474-4490.

[18] Lee, B., He, J., Chang, R.P. and Kanatzidis, M.G., 2012. All-solid-state dye-sensitized solar cells with high efficiency. *Nature*, 485(7399), pp.486-489.

[19] West, W., 1974. Proceedings of vogel centennial symposium. *Photogr. Sci. Eng*, 18, p.35.

[20] Zheng, X., Guo, J., Shi, Y., Xiong, F., Zhang, W.H., Ma, T. and Li, C., 2013. Low-cost and high-performance $CoMoS_4$ and $NiMoS_4$ counter electrodes for dye-sensitized solar cells. *Chemical Communications*, 49(83), pp.9645-9647.

[21] Ramasamy, K., Tien, B., Archana, P.S. and Gupta, A., 2014. Copper antimony sulfide ($CuSbS_2$) mesocrystals: a potential counter electrode material for dye-sensitized solar cells. *Materials Letters*, 124, pp.227-230.

[22] Baxter, J.B., 2012. Commercialization of dye-sensitized solar cells: Present status and future research needs to improve efficiency, stability, and manufacturing. *Journal of Vacuum Science & Technology A: Vacuum, Surfaces, and Films*, 30(2), p.020801.

[23] Wu, J., Li, Q., Fan, L., Lan, Z., Li, P., Lin, J. and Hao, S., 2008. High-performance polypyrrole nanoparticles counter electrode for dye-sensitized solar cells. *Journal of Power Sources*, 181(1), pp.172-176.

[24] Zhang, X., Chen, X., Zhang, K., Pang, S., Zhou, X., Xu, H., Dong, S., Han, P., Zhang, Z., Zhang, C. and Cui, G., 2013. Transition-metal nitride nanoparticles embedded in N-doped reduced graphene oxide: superior synergistic electrocatalytic materials for the counter electrodes of dye-sensitized solar cells. *Journal of Materials Chemistry A*, 1(10), pp.3340-3346.

[25] Choi, H., Kim, H., Hwang, S., Choi, W. and Jeon, M., 2011. Dye-sensitized solar cells using graphene-based carbon nano composite as counter electrode. *Solar Energy Materials and Solar Cells*, 95(1), pp.323-325.

[26] Velten, J., Mozer, A.J., Li, D., Officer, D., Wallace, G., Baughman, R. and Zakhidov, A., 2012. Carbon nanotube/graphene nanocomposite as efficient counter electrodes in dye-sensitized solar cells. *Nanotechnology*, 23(8), p.085201.

[27] Saito Y, Kitamura T, Wada Y, Yanagida S. Application of poly(3,4- ethylendioxythiophene) as counter electrode in dye-sensitized solar cells. Chemistry Letters 2002; 3:1060–1061.

[28] Ahmed, A.S., Xiang, W., Hu, X., Qi, C., Amiinu, I.S. and Zhao, X., 2018. Si_3N_4/MoS_2-PEDOT:PSS composite counter electrode for bifacial dye-sensitized solar cells. *Solar Energy*, 173, pp.1135-1143.

[29] Peng, S., Tian, L., Liang, J., Mhaisalkar, S.G., Ramakrishna, S., 2012. Polypyrrole nanorod networks/carbon nanoparticles composite counter electrodes for high-efficiency dyesensitized solar cells. ACS Appl. Mater. Interfaces 4, 397–404.

[30] Zheng, X., Xu, J., Yan, K., Wang, H., Wang, Z., Yang, S., 2014a. Space-confined growth of MoS_2 nanosheets within graphite: the layered hybrid of MoS_2 and graphene as an active catalyst for hydrogen evolution reaction. Chem. Mater. 26, 2344–2353.

[31] Zheng, X., Deng, J., Wang, N., Deng, D., Zhang, W.H., Bao, X., Li, C., 2014b. Podlike Ndoped carbon nanotubes encapsulating FeNi alloy nanoparticles: high-performance counter electrode materials for dye-sensitized solar cells. Angew. Chem. Int. Ed. 53, 1–6. A.S.A. Ahmed et al. *Solar Energy 173 (2018) 1135–1143*

[32] Chawarambwa, F.L., Putri, T.E., Attri, P., Kamataki, K., Itagaki, N., Koga, K. and Shiratani, M., 2021. Highly efficient and transparent counter electrode for application in bifacial solar cells. *Chemical Physics Letters*, 768, p.138369.

[33] Tevi, T., Saint Birch, S.W., Thomas, S.W. and Takshi, A., 2014. Effect of Triton X-100 on the double layer capacitance and conductivity of poly (3, 4-ethylenedioxythiophene): poly (styrenesulfonate)(PEDOT: PSS) films. *Synthetic metals*, 191, pp.59-65.

[34] Kavan, L., Yum, J.H. and Gratzel, M., 2011. Optically transparent cathode for dye-sensitized solar cells based on graphene nanoplatelets. ACS Nano 5: 165–172.

[35] Phillips, A.B., Subedi, K.K., Liyanage, G.K., Alfadhili, F.K., Ellingson, R.J. and Heben, M.J., 2020. Understanding and advancing bifacial thin film solar cells. *ACS Applied Energy Materials*, 3(7), pp.6072-6078.

[36] Xu, T., Kong, D., Tang, H., Qin, X., Li, X., Gurung, A., Kou, K., Chen, L., Qiao, Q. and Huang, W., 2020.Transparent MoS2/PEDOT composite counter electrodes for bifacial dye-sensitized solar cells. *ACS omega*, 5(15), pp.8687-8696.

[37] Kim, J.Y., Jung, J.H., Lee, D.E. and Joo, J., 2002. Enhancement of electrical conductivity of poly (3, 4-ethylenedioxythiophene)/poly (4-styrenesulfonate) by a change of solvents. *Synthetic Metals*, *126*(2-3), pp.311-316.

[38] Chen, J.G., Wei, H.Y. and Ho, K.C., 2007. Using modified poly (3, 4-ethylene dioxythiophene): Poly (styrene sulfonate) film as a counter electrode in dye-sensitized solar cells. *Solar Energy Materials and Solar Cells*, *91*(15-16), pp.1472-1477.

[39] So, S.H., Joo, K.K., Kim, B.R., Kim, B.K., Kim, S.C., Shin, C.D. and Yeo, I.S., 2014. Development of a liquid scintillator using water for a next generation neutrino experiment. *Advances in High Energy Physics*, *2014*.

[39] X. Wang, L. Zhi, K. Müllen, Nano Lett. 8 (2008) 323, https://doi.org/10.1021/ nl072838r.

[40] Kang, J.S., Kim, J., Kim, J.Y., Lee, M.J., Kang, J., Son, Y.J., Jeong, J., Park, S.H., Ko, M.J. and Sung, Y.E., 2018. Highly efficient bifacial dye-sensitized solar cells employing polymeric counter electrodes. *ACS applied materials & interfaces*, *10*(10), pp.8611-8620.

[41] Zhang, L., Chen, W., Wang, T., Li, Y., Ma, C., Zheng, Y. and Gong, J., 2021. Polyoxometalate modified transparent metal selenide counter electrodes for high-efficiency bifacial dye-sensitized solar cells. *Inorganic Chemistry Frontiers*, *8*(13), pp.3230-3237.

[42] Xia, J., Wang, Q., Xu, Q., Yu, R., Chen, L., Jiao, J., Fan, S. and Wu, H., 2020. High efficiency bifacial quasi-solid-state dye-sensitized solar cell based on $CoSe_2$ nanorod counter electrode. *Applied Surface Science*, *530*, p.147238.

[43] Lee, K.S., Lee, Y., Lee, J.Y., Ahn, J.H. and Park, J.H., 2012. Flexible and platinum-free dye-sensitized solar cells with conducting-polymer-coated graphene counter electrodes. *ChemSusChem*, *5*(2), pp.379-382.

[44] Ma, T., Fang, X., Akiyama, M., Inoue, K., Noma, H. and Abe, E., 2004. Properties of several types of novel counter electrodes for dye-sensitized solar cells. *Journal of Electroanalytical Chemistry*, *574*(1), pp.77-83.

[45] Xu, S., Luo, Y. and Zhong, W., 2011. Investigation of catalytic activity of glassy carbon with controlled crystallinity for counter electrode in dye-sensitized solar cells. *Solar energy*, *85*(11), pp.2826-2832.

[46] Xu, S., Luo, Y. and Zhong, W., 2011. Investigation of catalytic activity of glassy carbon with controlled crystallinity for counter electrode in dye-sensitized solar cells. *Solar energy*, *85*(11), pp.2826-2832.

[47] Wang, M., Anghel, A.M., Marsan, B., Cevey Ha, N.L., Pootrakulchote, N., Zakeeruddin, S.M. and Gratzel, M., 2009. CoS supersedes Pt as efficient electrocatalyst for triiodide reduction in dye-sensitized solar cells. *Journal of the American Chemical Society*, *131*(44), pp.15976-15977.

[48] Levy, R.B. and Boudart, M., 1973. Platinum-like behavior of tungsten carbide in surface catalysis. *science*, *181*(4099), pp.547-549.

[49] Wu, M., Lin, X., Wang, Y., Wang, L., Guo, W., Qi, D., Peng, X., Hagfeldt, A., Gratzel, M. and Ma, T., 2012. Economical Pt-free catalysts for counter electrodes of dye-sensitized solar cells. *Journal of the American Chemical Society*, *134*(7), pp.3419-3428.

[50] Kavan, L., Yum, J.H. and Gratzel, M., 2011. Optically transparent cathode for dye-sensitized solar cells based on graphene nanoplatelets. *Acs Nano*, *5*(1), pp.165-172.

[51] Murakami, T.N. and Gratzel, M., 2008. Counter electrodes for DSC: application of functional materials as catalysts. *InorganicaChimica Acta*, *361*(3), pp.572-580.

[52] Lee, K.S., Lee, Y., Lee, J.Y., Ahn, J.H. and Park, J.H., 2012. Flexible and platinum-free dye-sensitized solar cells with conducting-polymer-coated graphene counter electrodes. *ChemSusChem*, *5*(2), pp.379-382.